The *Arabidopsis* SUPPRESSOR OF AUXIN RESISTANCE Proteins Are Nucleoporins with an Important Role in Hormone Signaling and Development [W]

Geraint Parry,[1] Sally Ward,[1,2] Alex Cernac,[3] Sunethra Dharmasiri,[4] and Mark Estelle[5]

Department of Biology, Indiana University, Bloomington, Indiana 47405

Nucleocytoplasmic transport of macromolecules is regulated by a large multisubunit complex called the nuclear pore complex (NPC). Although this complex is well characterized in animals and fungi, there is relatively little information on the NPC in plants. The *suppressor of auxin resistance1* (*sar1*) and *sar3* mutants were identified as suppressors of the *auxin-resistant1* (*axr1*) mutant. Molecular characterization of these genes reveals that they encode proteins with similarity to vertebrate nucleoporins, subunits of the NPC. Furthermore, a SAR3–green fluorescent protein fusion protein localizes to the nuclear membrane, indicating that SAR1 and SAR3 are *Arabidopsis thaliana* nucleoporins. Plants deficient in either protein exhibit pleiotropic growth defects that are further accentuated in *sar1 sar3* double mutants. Both *sar1* and *sar3* mutations affect the localization of the transcriptional repressor AXR3/INDOLE ACETIC ACID17, providing a likely explanation for suppression of the phenotype conferred by *axr1*. In addition, *sar1 sar3* plants accumulate polyadenylated RNA within the nucleus, indicating that SAR1 and SAR3 are required for mRNA export. Our results demonstrate the important role of the plant NPC in hormone signaling and development.

INTRODUCTION

Nucleocytoplasmic transport is an essential process in eukaryotic organisms (Gorlich and Kutay, 1999; Weis, 2003). Protein and RNA molecules move between the nuclear and cytoplasmic compartments through pores that lie at invaginations of the nuclear membrane. The nuclear pore is composed of a set of membrane-bound anchor proteins and a protein complex that lies within the space occupied by the pore (Hetzer et al., 2005). This nuclear pore complex (NPC) is a large conglomerate composed of protein subcomplexes that are repeated in eightfold radial symmetry around a central channel (Vasu and Forbes, 2001). The NPC has been studied in some detail in both animals and yeast but is poorly characterized in plants. Many general features of the NPC, as well as the constituent protein complexes, are conserved among all eukaryotes that have been investigated (Bapteste et al., 2005). Recent studies have begun to define which protein subcomplexes are responsible for the movement of specific molecules into and out of the nucleus. One such complex, called the NUP107–120 complex in animals and the NUP84 complex in yeast, plays a central role in NPC function (Siniossoglou et al., 2000; Bai et al., 2004; Loiodice et al., 2004).

Comprehensive analysis of the NUP107–120 complex has defined at least nine members (Lutzmann et al., 2002; Loiodice et al., 2004). Its central importance is highlighted by the fact that when the complex is depleted from *Xenopus laevis* egg extracts, the reconstituted nuclei are devoid of nuclear pores (Harel et al., 2003; Walther et al., 2003). Furthermore, mutation of individual members of this complex in human cell lines and in yeast results in smaller nuclei that have severe defects in mRNA export (Siniossoglou et al., 1996; Vasu et al., 2001; Bai et al., 2004).

Transport of molecules through the NPC is mediated by karyopherin proteins. Individual members of this large protein family can facilitate nuclear import (importins) or export (exportins), and their activity requires interaction with the small GTPase Ran (Harel and Forbes, 2004; Mosammaparast and Pemberton, 2004).

Although relatively few studies have been performed, the mechanism of nucleocytoplasmic transport appears to be conserved between plants and other eukaryotes (Merkle, 2003; Meier, 2005). The *Arabidopsis thaliana* proteome contains proteins similar to many of those involved in metazoan and yeast nucleocytoplasmic transport, including karyopherin proteins. The *HASTY* and *PAUSED* genes encode plant homologs of exportin5 and exportinT, respectively (Bollman et al., 2003; Hunter et al., 2003; Li and Chen, 2003). HASTY interacts with the small GTPase Ran in a yeast two-hybrid assay, localizes to the nuclear periphery, and is involved in nuclear processing of certain microRNAs (miRNAs) (Bollman et al., 2003; Park et al., 2005). Expression of *PAUSED* in *Saccharomyces cerevisiae* rescues a deficiency in exportinT, whereas *paused* mutant plants accumulate transfer RNAs in the nucleus (Hunter et al., 2003; Park et al., 2005). These results indicate that HASTY and PAUSED play a role in the nuclear export of RNA. Plants deficient for either of these proteins exhibit a pleiotropic phenotype that is characterized by

defects in phase change (Telfer and Poethig, 1998; Hunter et al., 2003; Li and Chen, 2003). The precise explanation for this phenotype is not known, although it is presumably related to a defect in RNA processing and transport.

The LOS4 protein is a DEAD box RNA helicase that is localized to the nuclear rim (Gong et al., 2005). Accumulation of poly(A) RNA in the nuclei of *los4* plants suggests that it is required for the movement of mRNA into the cytoplasm (Gong et al., 2005). Interestingly, like the *hasty* and *paused* mutants, *los4* mutants exhibit early flowering.

The *Arabidopsis MOS3* and *MOS6* (for *MODIFIER OF SNC1*) genes were identified from a mutant screen for suppressors of gain-of-function *snc1* (for *suppressor of npr1-1, constitutive*) plants (Palma et al., 2005; Zhang and Li, 2005). *SNC1* is a disease resistance gene that when mutated in a predicted regulatory region leads to constitutive activation of the disease resistance response. MOS3 is a homolog of vertebrate nucleoporin NUP96, and consistent with its proposed role, MOS3–green fluorescent protein (GFP) localizes to the nuclear periphery (Zhang and Li, 2005). Human NUP96 and its yeast homolog NUP145C are members of the NUP107–120 subcomplex, suggesting that this large subcomplex is also present in plants. The *MOS6* gene encodes the importin AtImpα3 (Palma et al., 2005). Single *mos3* and *mos6* mutants exhibit increased susceptibility to certain pathogens (Palma et al., 2005; Zhang and Li, 2005). It is unclear at present how the NPC and the nuclear transport machinery specifically affect the disease resistance response. However *mos3* and/or *mos6* may alter the transport of disease-specific macro-molecules or reduce activity in other functions of the putative plant NUP107–120 complex (Palma et al., 2005; Zhang and Li, 2005).

The *Arabidopsis auxin-resistant1* (*axr1*) mutants were originally isolated in a screen for auxin-resistant seedlings (Lincoln et al., 1990). Subsequent analysis demonstrated that AXR1 is a subunit in the RUB-activating enzyme, the first enzyme in a pathway that conjugates the ubiquitin-related protein RUB to members of the cullin family (del Pozo and Estelle, 1999; del Pozo et al., 2002; Parry and Estelle, 2004). Cullin proteins are components of several distinct families of ubiquitin protein ligases (E3), including the well-characterized SCF complexes (Deshaies, 1999). In general, E3 enzymes promote the attachment of ubiquitin to diverse proteins, typically resulting in their degradation by the proteasome (Moon et al., 2004). The *axr1* mutants are auxin-resistant because the RUB conjugation pathway is required for the normal function of the E3 SCF^{TIR1} and related SCFs (del Pozo et al., 2002). These SCFs promote the auxin-dependent degra-dation of a family of transcriptional repressors called the Aux/IAA proteins (Gray et al., 1999, 2001). This degradation is likely to occur within the nucleus, because both SCF^{TIR1} and the Aux/IAA proteins are present in this compartment. In *axr1* plants, the Aux/IAAs accumulate, presumably in the nucleus, and repress auxin-regulated transcription, resulting in decreased auxin response.

To further understand the function of the AXR1 protein, we have screened for extragenic suppressors of the *axr1* mutants. Previously, we described the characterization of a second-site suppressor of *axr1* called *suppressor of auxin resistance1* (*sar1*) (Cernac et al., 1997). Here, we report the identification of another suppressor named *sar3* and the molecular characterization of both *SAR1* and *SAR3*. Surprisingly, we find that *SAR1* and *SAR3*

encode putative nucleoporins of the NUP107–120 subcomplex. Our results suggest that defects in this complex restore partial auxin sensitivity to *axr1* mutants by affecting the translocation of the Aux/IAA proteins into the nucleus. Furthermore, the loss of both SAR1 and SAR3 results in a severe growth phenotype and the accumulation of poly(A)$^+$ RNA in the nucleus.

RESULTS

Identification of New Suppressors of the *axr1* Mutant

The *axr1* mutants are auxin-resistant and exhibit a pleiotropic phenotype consistent with an overall reduction in auxin response (Lincoln et al., 1990; Leyser et al., 1993). In a previous report, we described the isolation of the *sar1* mutant (Cernac et al., 1997). This recessive mutation restores auxin response to the roots of *axr1* seedlings. Subsequent analysis indicated that the *sar1* mutation suppresses most aspects of the phenotype conferred by *axr1*. In addition, *sar1* mutants have a novel phenotype that is independent of *AXR1* (Cernac et al., 1997).

To identify additional *axr1* suppressors, we performed a new screen, this time focusing on the *axr1* hypocotyl phenotype. When grown at 29°C in the light, ecotype Columbia (Col-0) seed-lings have an elongated hypocotyl compared with seedlings grown at a lower temperature (Gray et al., 1998). By contrast, *axr1* seedlings do not exhibit this auxin-dependent response. We grew mutagenized *axr1-3* seedlings at the higher temperature and identified 25 lines with taller hypocotyls. Genetic analysis revealed that two lines, isolated from independent pools of mutagenized seeds, carried recessive alleles of one locus, and we called these lines *sar3-1* and *sar3-2*.

The *sar3-1* Mutation Suppresses Most Aspects of the Phenotype Conferred by *axr1* and Results in Early Flowering

Consistent with our mutant screen, the hypocotyls of *sar3-1 axr1-3* plants are longer than those of *axr1-3* plants when grown at 29°C (Figure 1A). Furthermore, *sar3-1* partially suppresses other aspects of the phenotype conferred by *axr1*, including auxin-resistant root growth and a decrease in auxin-induced lateral root formation (Figure 1B). The roots of *axr1* mutants are also resistant to methyl jasmonate (Tiryaki and Staswick, 2002), and *sar3-1* partially re-stores this response (see Supplemental Figure 1 online).

In addition to defects in auxin growth responses, the *axr1* mutants are deficient in auxin-regulated transcription, including expression of the *Aux/IAA* genes (Abel et al., 1995; Timpte et al., 1995). To determine whether *sar3-1* affects auxin induction of the *Aux/IAA* genes, we measured *IAA1* and *IAA5* RNA levels in response to auxin. The data in Figure 1C show that *sar3-1* par-tially restores auxin induction of both *IAA1* and *IAA5* in the *axr1-3* mutant. Similar results were obtained with the *sar1* mutant (Cernac et al., 1997).

We next investigated the affects of *sar3* on development in both *axr1* and *AXR1* backgrounds (Figure 1D, Table 1). In general, *sar3* and *sar3 axr1* plants are very similar in appearance. The primary root is shorter than in the wild type and produces fewer lateral roots (Table 1). Most striking, both single and double
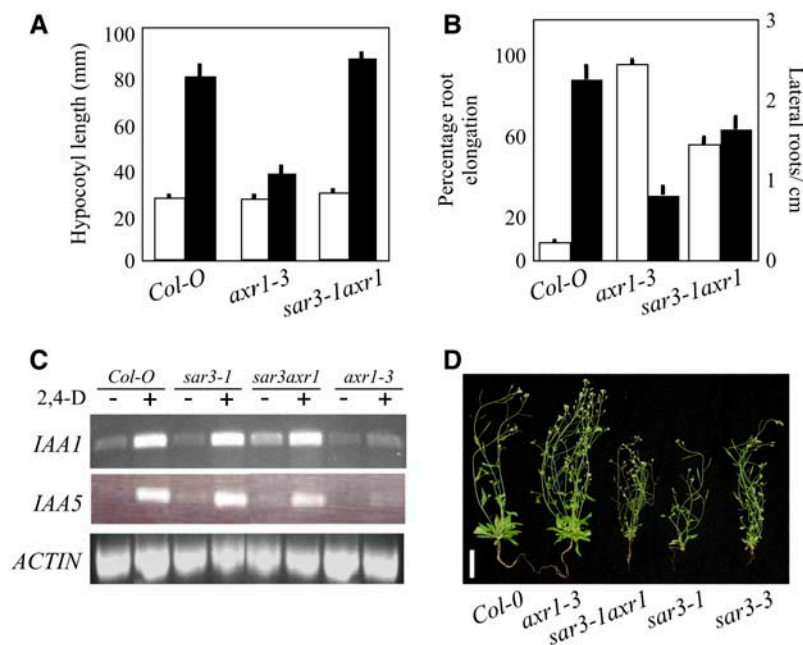
Figure 1. The *sar3-1* Mutation Suppresses Aspects of the Phenotype Conferred by *axr1*.

(A) Wild-type and mutant seedlings were grown for 9 d in the light at 22°C (white bars) or 29°C (black bars). Error bars represent SD ($n = 20$ or greater).
(B) Root elongation (white bars) of wild-type and mutant seedlings grown on 0.16 μM 2,4-D. Four-day-old seedlings were transferred to medium with hormone, and growth was measured after 3 d. Values are expressed as percentages of root growth of each genotype on medium without hormone ($n = 12$ or greater). Black bars represent lateral roots on 10-d-old seedlings grown on ATS medium ($n = 10$ or greater). Error bars represent SE.
(C) RT-PCR on RNA extracted from 10-d-old wild-type and mutant seedlings treated with or without 20 μM 2,4-D for 1 h. Primers for the *IAA1* and *IAA5* genes were used to demonstrate auxin-induced gene expression. Primers from *ACTIN2* were used as a control.
(D) Appearance of 5-week-old wild-type and mutant plants. Bar = 5 cm.

mutants flower significantly earlier than wild-type plants and are much smaller and less robust throughout their life cycle (Figure 1D, Table 1). Overall, the phenotype conferred by *sar3* is very similar to that conferred by *sar1* (Cernac et al., 1997). These findings suggest that the two genes have related functions in hormone response and development.

The *sar1* and *sar3* Mutations Partially Suppress the *rce1* Mutation

The AXR1 protein is a subunit of the heterodimeric E1 enzyme that functions in the RUB conjugation pathway. The next step in the pathway is a RUB-conjugating enzyme (E2) called RCE1 (del Pozo

and Estelle, 1999; Dharmasiri et al., 2003). Like *axr1*, mutations in *rce1* lead to multiple auxin-related defects (Dharmasiri et al., 2003). To determine whether the *SAR* genes have a general effect on RUB conjugation, we generated *sar1 rce1* and *sar3 rce1* double mutants and characterized their phenotypes. Both *sar1* and *sar3* partially suppress auxin resistance conferred by *rce1* (Figure 2A). The *sar3 rce1* plants are more sensitive to auxin than are *sar1 rce1* plants, indicating that *sar3* suppresses this phenotype of *rce1* better than *sar1*.

Mutant *rce1* plants are shorter than wild-type plants (Dharmasiri et al., 2003), and both *sar1-1* and *sar3-1* partially suppress this defect (Figure 2B). In general, both the *sar1 rce1* and *sar3 rce1* mutants are similar to the *sar1* and *sar3* single mutants, with a

Table 1. Phenotypes of Wild-Type and Mutant Plants

| Characteristic	Col-0	*axr1-3*	*sar3-1*	*sar3 axr1*
Primary root at 6 d (mm)	24.8 ± 0.7	32.5 ± 1.1	18.5 ± 2.1	20.8 ± 1.1
Lateral roots per centimeter of primary root at 10 d	2.2 ± 0.2	0.81 ± 0.1	1.63 ± 0.2	1.69 ± 0.1
Bolting time (d)	25.0 ± 0.2	25.1 ± 0.2	15.7 ± 0.1	16.0 ± 0.1
Rosette leaves at bolt	10.7 ± 0.2	10.7 ± 0.2	6.2 ± 0.1	6.1 ± 0.1
Primary inflorescence (cm)	38.4 ± 0.95	35.1 ± 1.0	27.1 ± 1.3	27.0 ± 1.0
Branches per centimeter of primary inflorescence	0.12 ± 0.01	0.19 ± 0.01	0.12 ± 0.01	0.14 ± 0.01
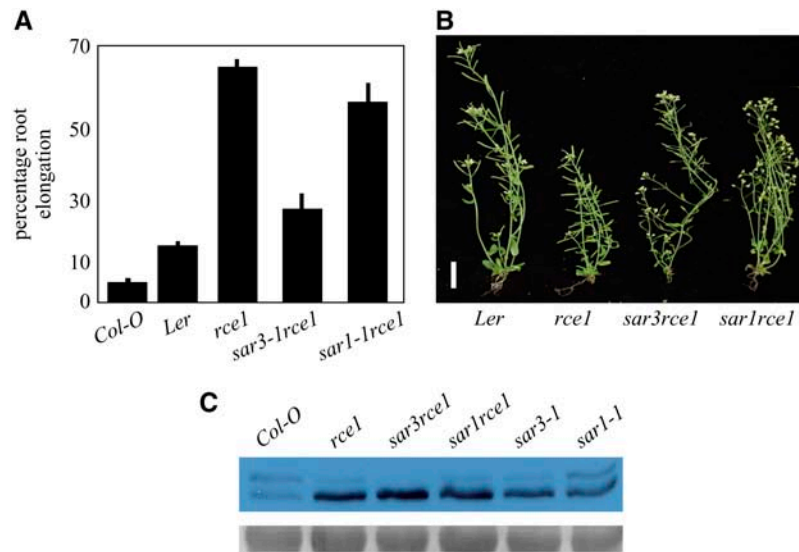
Figure 2. The *sar1* and *sar3* Mutations Suppress Auxin Resistance Exhibited by *rce1* Plants.

(A) Root elongation of wild-type and mutant seedlings grown on 0.16 μM 2,4-D. The experiment was performed as described for Figure 1B. Student's *t* test indicated that the values for *rce1* and *sar1 rce1* are significantly different (P < 0.05). Error bars represent SE (*n* = 10 or greater). *Ler*, Landsberg *erecta*.
(B) Phenotypes of 5-week-old wild-type and mutant plants. Bar = 2 cm.
(C) Immunoblot using anti-CUL1 antibody on total protein extracted from floral tissue. Arrows indicate RUB-modified (top) and unmodified (bottom) forms of CUL1. The bottom gel shows an unknown nonspecific band used as a loading control.

reduction in floral bud size, a decrease in stem thickness, and a decrease in silique size (see Supplemental Figure 2 online).

The only known substrates of the RUB modification pathway are the cullin proteins. In the *axr1* and *rce1* mutants, the level of RUB-modified CUL1 is reduced, resulting in a decrease in SCF function (del Pozo et al., 2002; Dharmasiri et al., 2003). To determine whether the *sar1* and *sar3* mutations directly affect the RUB conjugation pathway, we examined the level of RUB-CUL1 in *sar1-1* and *sar3-1* plants. As shown previously, the relative level of RUB-modified CUL1 is drastically decreased in the *rce1* mutant (Figure 2C) (Dharmasiri et al., 2003). Neither the *sar1-1* nor the *sar3-1* mutation increased the level of RUB-CUL1 in an *rce1* background (Figure 2C). Thus, suppression by *sar1* and *sar3* does not directly involve changes in the RUB conjugation pathway.

SAR3 Is Related to Vertebrate NUP96

To gain further insight into the function of *SAR3*, we cloned the gene using a map-based strategy. We crossed *sar3-1* (Col-0) with ecotype Landsberg *erecta* and recovered homozygous *sar3-1* plants from the resulting F2 population. After an analysis of 680 plants, the *sar3* mutation was mapped to a 140-kb region at the bottom of chromosome 1 on BAC F23A5. While this work was in progress, we learned that an early-flowering mutant called *precoz* (*pre*) had also been mapped to the same region (C. Alonso-Blanco, I. Ausin, L. Ruiz-Garcia, and J.M. Martinez-Zapater, unpublished data) and encoded the At1g10860 protein. Because both *sar3-1* and *pre* are early-flowering, we sequenced the *At1g10860* gene from *sar3-1* and *sar3-2* plants. This analysis revealed the presence of a single base pair deletion at position

1103 within the predicted second exon of the *sar3-1* gene. The identical lesion was detected in *sar3-2*, even though these lines were isolated independently. This change introduces a premature stop codon 150 bp downstream from the site of the mutation (Figure 3A). To verify that this mutation is responsible for the phenotype conferred by *sar3-1*, we obtained a T-DNA insertion line (*sar3-3*) from the Salk Institute Genomic Laboratory T-DNA collection (SALK_109959) (Alonso et al., 2003). The T-DNA insertion is within intron 4 at position 3570 with respect to the ATG. Like *sar3-1*, *sar3-3* plants have a shorter root than wild-type plants and flower early. In addition, the aerial phenotype of *sar3-3* plants is indistinguishable from that of *sar3-1*, confirming that At1g10860 is *SAR3* (Figure 1C). This gene was also identified in a screen for suppressors of the *snc1* mutation and designated *MOS3* (Zhang and Li, 2005).

To determine the pattern of *SAR3* gene expression, we performed RT-PCR using RNA from a variety of tissues. We found that *SAR3* is expressed in representative tissues throughout the plant (Figure 3B). We also determined the effects of the *sar3-1* and *sar3-3* mutations on the *SAR3* transcript. Figure 3B shows that the *sar3-1* mutant produces a full-length transcript, whereas in *sar3-3* we detected a partial transcript. Because both alleles may produce a truncated protein, it is not clear whether either mutation is a functional null.

As reported previously, *SAR3/MOS3* is a unique gene in *Arabidopsis* and encodes a protein with similarity to human NUP96 (Zhang and Li, 2005). However, unlike that previous study, our analysis indicated that the N terminus of the SAR3/MOS3 protein is also related to the C terminus of a different human nucleoporin, NUP98. This finding can be explained by the fact that in vertebrates, both NUP96 and NUP98 are produced by the
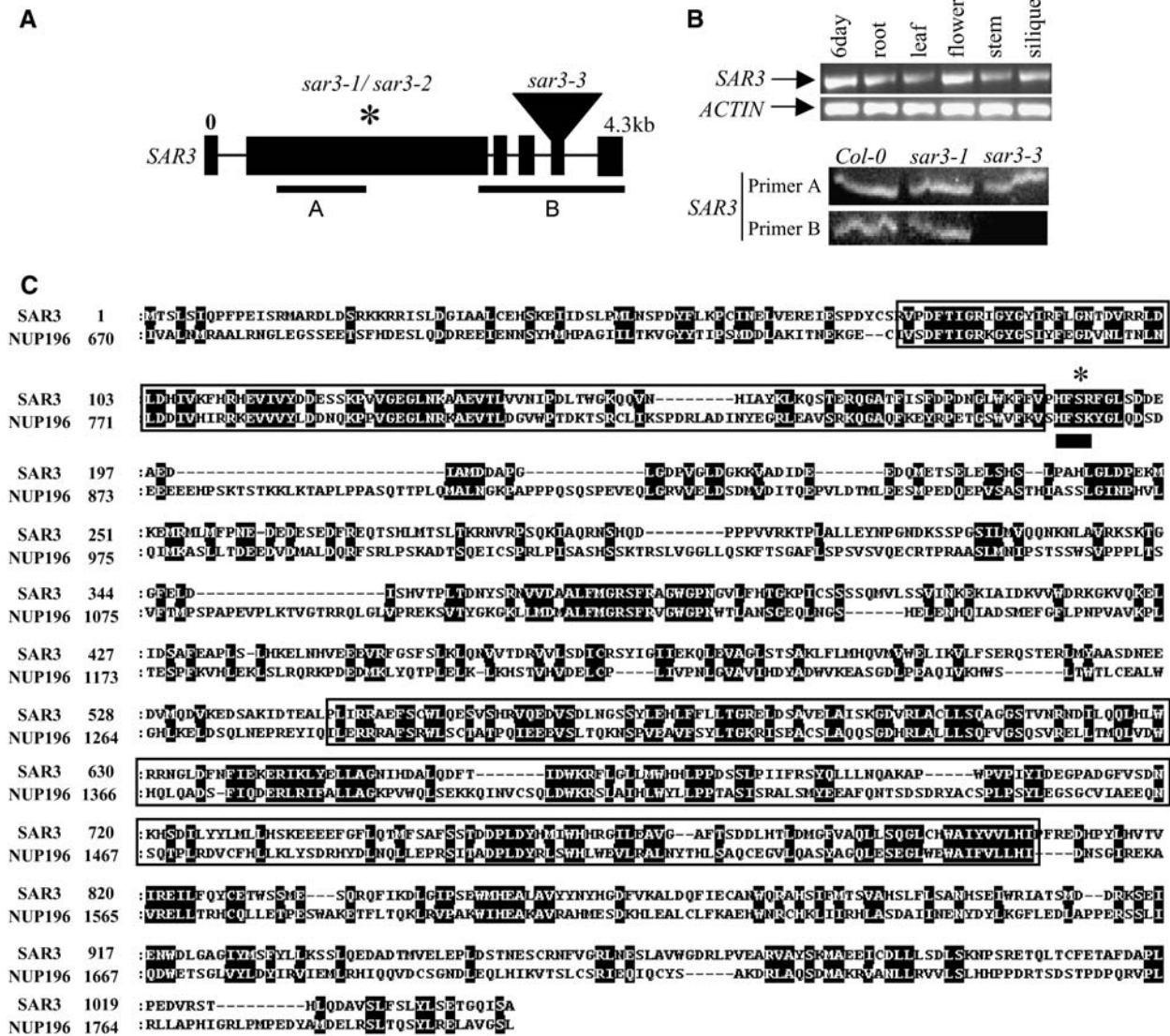
Figure 3. SAR3 Is Similar to Vertebrate NUP96.

(A) Structure of the *SAR3* gene. Boxes represent exons. The asterisk denotes the position of deletions in *sar3-1* and *sar3-2*; the position of the T-DNA insertion in *sar3-3* is represented by an inverted triangle. Lines A and B correspond to regions amplified from the cDNA by primers used in **(B)**.
(B) RT-PCR of *SAR3* transcript using RNA from a variety of tissues and in *sar3* mutant alleles using internal primers within the *SAR3* and *ACTIN2* genes. Roots are from 12-d-old seedlings, and leaves are rosette leaves from 27-d-old plants. Regions amplified by primers A and B are represented in **(A)**.
(C) Alignment of the amino acid sequence of SAR3 (1046 residues) and the C-terminal 1130 residues from human NUP196 (residues 670 to 1800). This sequence represents the C-terminal 196 amino acids of the human NUP98 protein and the entire sequence of human NUP96. The site of autoproteolytic cleavage in NUP196 is underlined. The asterisk denotes the first amino acid (S) of NUP96. Boxed regions have >30% identity. Black shading denotes identical residues.

posttranslational processing of a larger precursor protein called NUP196. The N-terminal 864 amino acids of NUP196 form NUP98, and the C-terminal 920 amino acids form NUP96 (Fontoura et al., 1999). We found that SAR3/MOS3 shares 22% identity and 40% similarity with the C-terminal 1130 amino acids of NUP196 (Figure 3C). At its N terminus, SAR3/MOS3 is 45% identical to NUP196, and for a stretch of 336 amino acids in the center of the protein, the identity is >30% (Figure 3C). SAR3 appears to encompass the entire NUP96 protein sequence as well as the C-terminal 196 amino acids of NUP98. The region of similarity includes the well-

conserved site of autoproteolysis (Figure 3C). SAR3 also shares sequence similarity with NUP145 from *Saccharomyces cerevisiae* (see Supplemental Figure 3 online). This protein is homologous with human NUP196 and also undergoes processing to generate two distinct nucleoporins called NUP145N and NUP145C (Teixeira et al., 1997, 1999; Rosenblum and Blobel, 1999). Although NUP96 and NUP145C have a low level of similarity (Fontoura et al., 1999), several studies have demonstrated that these nucleoporins reside within equivalent protein complexes and are likely to have similar functions (Vasu et al., 2001; Lutzmann et al., 2002).

NUP96 localizes to the nuclear periphery in human cell lines (Enninga et al., 2003). To determine whether SAR3 is also localized to the nuclear periphery, we generated transgenic plants that express a SAR3-GFP translational fusion under the control of the cauliflower mosaic virus *35S* promoter. We isolated 25 independent transgenic lines in a Col-0 background and observed no obvious phenotypic changes in these plants (Figure 4A). We then crossed the *35S:SAR3-GFP* transgene into *sar3-1* plants and identified homozygous *sar3-1* plants carrying the transgene among the F2 progeny. These plants have a nearly wild-type phenotype, confirming that SAR3-GFP is functional (Figure 4A). The localization of SAR3-GFP was assessed by confocal microscopy. The results shown in Figure 4B demonstrate that SAR3-GFP was clearly localized to the nuclear periphery in cells of the root tip and the root elongation zone (Figure 4B). Considered together with its similarity to NUP96, this GFP localization strongly suggests that SAR3 is present within the NPC. Similar results have been obtained with lines expressing a MOS3-GFP transgene (Zhang and Li, 2005).

The *SAR1* Gene Encodes Another Nucleoporin, NUP160

Previously, we had mapped *SAR1* to chromosome 1 between markers *nga280* and *nga248* (Cernac et al., 1997). Further fine-

Figure 4. SAR3-GFP Is Localized to the Nuclear Periphery.

(A) Rosettes of 25-d-old wild-type and *sar3-1* plants with or without the *35S:SAR3-GFP* transgene. Bars = 2 cm.
(B) Confocal images of cells from the root tip (left) and the root elongation zone (right) from Col-0 *35S:SAR3-GFP*. Green signal represents GFP expression, and cell walls are stained with propidium iodide.

mapping resolved this interval to a 180-kb region that includes *At1g33410*, predicted to encode a protein related to the vertebrate nucleoporin NUP160. Given the similarity between the phenotypes conferred by *sar3* and *sar1*, this gene was a good candidate for *SAR1*. Sequence analysis of *At1g33410* in *sar1-1* plants revealed a point mutation at position 3403 that introduces a stop codon in the 11th exon of the gene (Figure 5A). Our previous study identified two additional *sar1* alleles. The *sar1-2* mutation has a phenotype similar to that of *sar1-1*, whereas *sar1-3* has a weaker phenotype (Cernac et al., 1997). We sequenced *At1g33410* in these lines and found that *sar1-2* contains a mutation at the junction between intron 4 and exon 5, whereas *sar1-3* has a mutation within intron 21 of the gene. We subsequently obtained a T-DNA allele with an insertion within *At1g33410* (*sar1-4*) from the Salk collection (SALK_126801) (Alonso et al., 2003). We used PCR to identify a line homozygous for *sar1-4* and subsequently verified by sequencing that the T-DNA insertion is within exon 17 of the gene at position 5652 with respect to the ATG. The *sar1-4* mutant displays the same aerial phenotype as *sar1-1* (Figure 5B), indicating that the defect in *At1g33410* is responsible for the phenotype conferred by *sar1*.

Like *SAR3*, the *SAR1* gene is expressed throughout the plant (Figure 5C). RT-PCR analysis shows that the *sar1-1* allele produces normal levels of transcript. However, in *sar1-4* plants, we could identify an RT-PCR product only using primers that are 5′ of the T-DNA insertion site (Figure 5C). Because it is possible that *sar1-4* produces a truncated protein, it is not clear whether any of the *sar1* alleles are nulls.

SAR1 is a large protein of 1500 amino acids that is not related to any other *Arabidopsis* protein. Along its entire length, SAR1 exhibits 14% identity and 31% similarity with the vertebrate nucleoporin NUP160. However, a C-terminal stretch of 400 amino acids in these two proteins shares 23% identity and 40% similarity (Figure 5D). These results, together with the similarity between the phenotypes conferred by *sar3* and *sar1*, suggest that SAR1 is the *Arabidopsis* homolog of NUP160. A recent analysis of the NPC among various eukaryotes also proposed that At1g33410 is a homolog of human NUP160 (Bapteste et al., 2005).

Defects in Both *SAR1* and *SAR3* Result in a Severe Phenotype

To learn more about the genetic and functional relationships between the SAR1 and SAR3 proteins, we generated *sar1 sar3* double mutant plants. Because we had difficulty generating a fertile double mutant line, we initially identified plants that were homozygous for *sar1* and heterozygous for *sar3*. These plants were similar to *sar1* or *sar3* single mutants (Figure 6A). Among the progeny of these plants, we identified *sar1 sar3* double mutants with a variety of significant growth defects. The phenotype of the double mutants was somewhat variable, but for the purpose of description, we divided them into two broad classes of approximately equal size. Class A plants lack pigment and die as seedlings. The most severely affected seedlings have two cotyledon-like structures but do not develop leaves or a root (Figure 6C). Other class A seedlings develop very small leaves
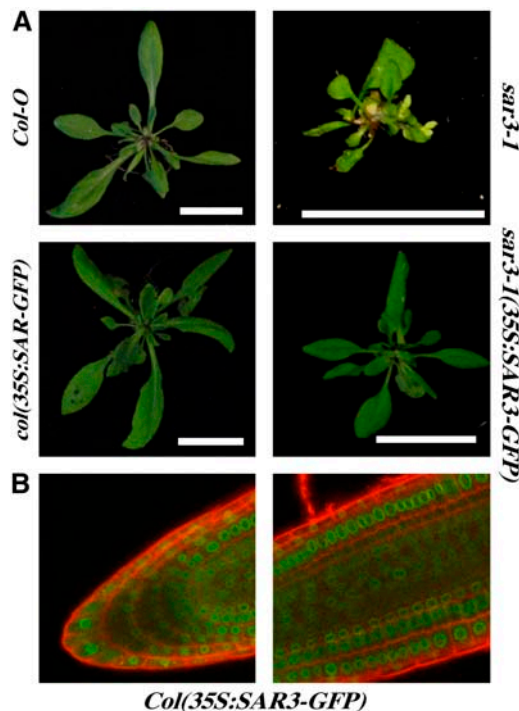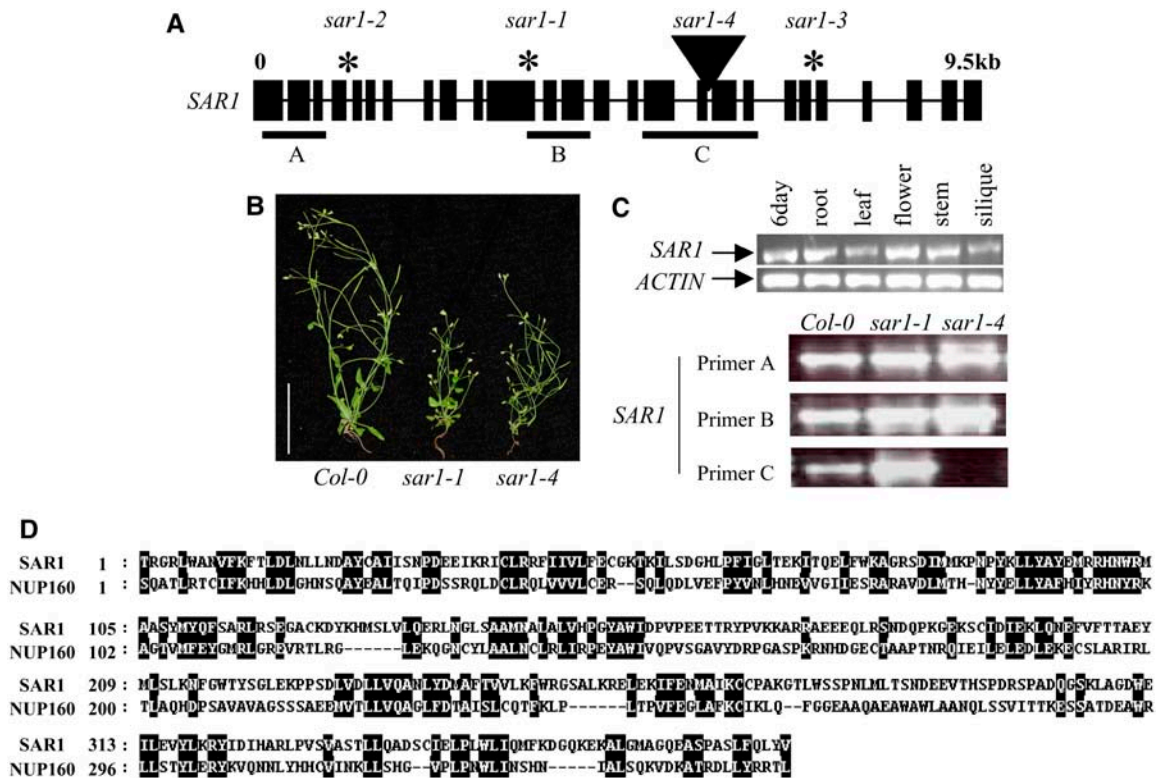
Figure 5. SAR1 Is Similar to Vertebrate NUP160.

(A) Structure of the *SAR1* gene. Boxes represent exons. Asterisks denote the positions of missense mutations in *sar1-1*, *sar1-2*, and *sar1-3*. The position of the T-DNA insertion in *sar1-4* is represented by an inverted triangle. Lines A to C correspond to regions amplified from the cDNA by primers used in **(C)**.
(B) Phenotypes of 5-week-old wild-type and *sar1* plants. Bar = 10 cm.
(C) RT-PCR of *SAR1* from a variety of tissue types and in *sar1* mutant alleles using internal primers within the *SAR1* and *ACTIN2* genes. Tissues are as described for Figure 3B. Regions amplified by primers A to C are shown in **(A)**.
(D) Alignment of amino acid sequence from SAR1 (residues 1028 to 1406) and human NUP160 (residues 962 to 1316). Black shading denotes identical residues.

but do not form a root and remain extremely small (Figure 6C). Class B plants develop a small root and misshapen leaves but remain small and undergo very early floral transition (Figure 6B). Typically, the primary inflorescence is similar to the wild type in appearance, but subsequent inflorescences are much shorter, giving the plants a short, bushy appearance (Figure 6D). These plants produce little or no seed.

An examination of *sar1 sar3* flowers provides an explanation for the infertility of these plants. As shown in Figure 6E, the gynoecium is reduced in these flowers and the anthers are poorly developed, forming very few if any pollen grains. Furthermore, these plants have a severe defect in inflorescence meristem function. In wild-type plants, flowers develop at regular intervals along the stem with a spiral phyllotaxy (Figure 6F). By contrast, in *sar1-1* and *sar3-1* single mutants, 35 to 40% of the flowers are irregularly spaced, causing the siliques to form in groups (Figure 6G). In *sar1 sar3* plants, the regular spacing of siliques is almost completely absent and ~80% of the siliques are grouped together (Figure 6H). This is indicative of a severe defect in the timing of floral meristem initiation.

sar1 sar3 Plants Are Deficient in mRNA Export

In vertebrate and yeast cells, defects in the NUP107–120 complex result in the accumulation of mRNA within the nucleus (Fabre et al., 1994; Vasu et al., 2001). A similar defect was observed in the *los4* mutant of *Arabidopsis* (Gong et al., 2005). To determine the effect of the *sar* mutants on mRNA localization, we performed in situ localization of poly(A) RNA (Fabre et al., 1994; Vasu et al., 2001; Boehmer et al., 2003; Gong et al., 2005). Small leaves (<5 mm) from wild-type and *sar1 sar3* plants grown at 22°C were fixed, labeled with a fluorescein-labeled poly(T) probe, and examined by confocal microscopy. In Col-0 leaves, a faint fluorescein signal could be observed both in the elongated cells adjacent to the midvein and also in the smaller cells between the midvein and the leaf margin (Figure 7). This is a similar result to that observed in leaves from the C24 *Arabidopsis* ecotype (Gong et al., 2005). In *sar1 sar3* leaves, we observed a much stronger fluorescent signal in the nuclei of both cell types (Figure 7). These results indicate that mRNA accumulates to higher levels in the nuclei of *sar1 sar3* cells than in wild-type cells.
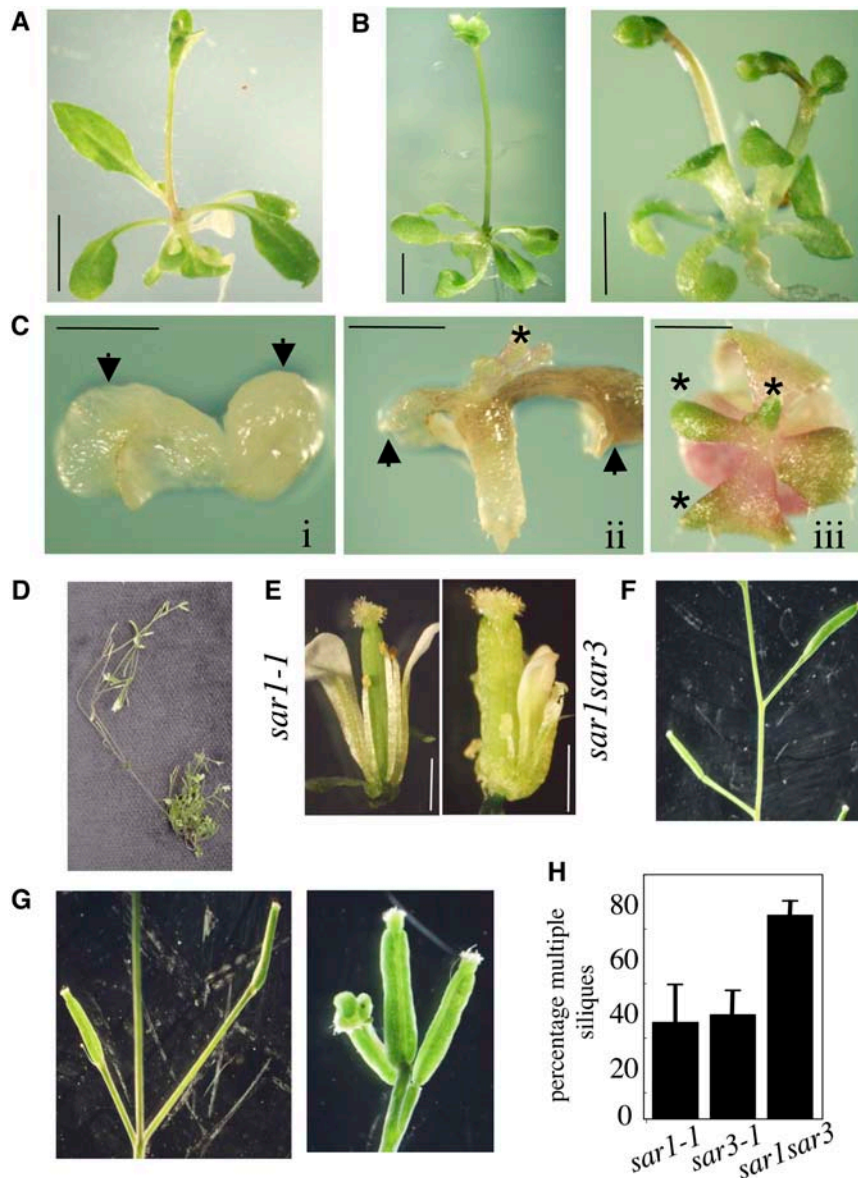
Figure 6. Loss of Both SAR1 and SAR3 Results in Severe Defects in Development.

(A) Phenotype of a 19-d-old plant homozygous for *sar1-1* and heterozygous for *sar3-1*. Bar = 5 mm.

(B) Examples of class B *sar1-1 sar3-1* mutants. These are the most robust double mutant plants. Bars = 2 mm.

(C) Examples of class A *sar1-1 sar3-1* seedlings. Arrows in (i) and (ii) show positions of cotyledons, and asterisks in (ii) and (iii) show locations of abortive true leaves. Bars = 1 mm.

(D) Phenotype of a 45-d-old *sar1-1 sar3-1* plant exhibiting a long primary inflorescence and numerous short secondary inflorescences.

(E) Representative flowers from *sar1-1* and *sar1-1 sar3-1* plants. Bars = 1 mm.

(F) Regular spacing of siliques in a wild-type plant.

(G) Examples of the irregular spacing of siliques that occurs in *sar1* or *sar3* single mutants (left) and *sar1-1 sar3-1* double mutants (right).

(H) Proportion of total siliques that are irregularly spaced in *sar1-1*, *sar3-1*, and *sar1-1 sar3-1* mutant plants. Measurement from wild-type plants is omitted, because these do not develop any irregularly spaced siliques. Error bars represent SE (*n* = 7 or greater).

Localization of the Aux/IAA Protein IAA17 Is Altered in *sar1* and *sar3* Mutants

The *axr1* mutants are deficient in auxin response because reduced levels of RUB-CUL1 affect the function of SCF[TIR1] and related SCF complexes. This defect results in the stabilization of the Aux/IAA proteins, repressors of auxin-regulated transcription (Dharmasiri and Estelle, 2004). To assess the effects of *sar1-1* on Aux/IAA degradation, we introduced the *HS:AXR3NT-GUS* transgene into mutant plants. This construct has been used to examine
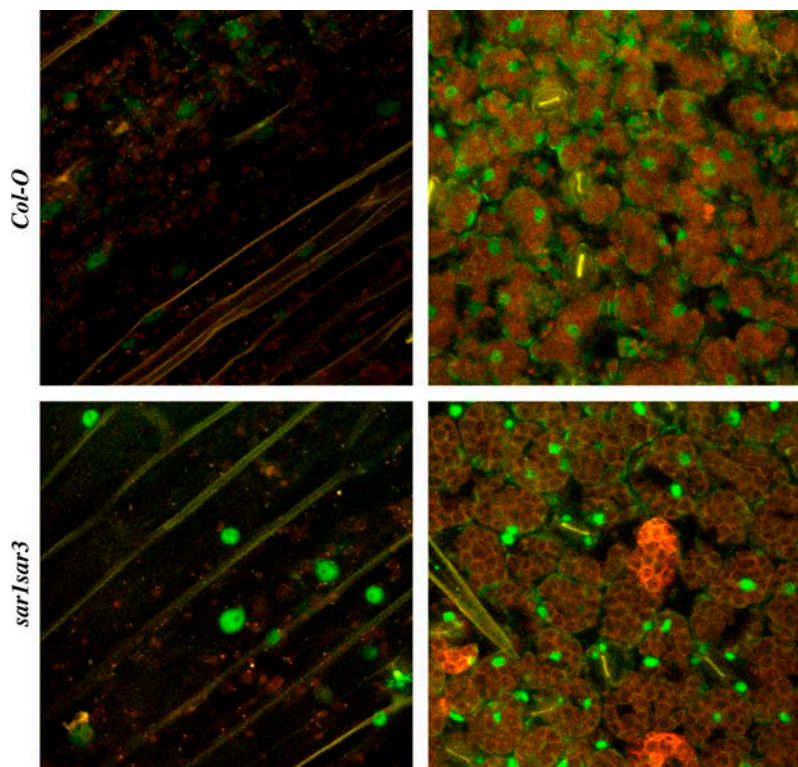
Figure 7. mRNA Accumulates in the Nuclei of *sar1-1 sar3-1* Cells.

Small leaves (<5 mm) from wild-type Col-0 and *sar1-1 sar3-1* plants were fixed and probed with a poly(dT) fluorescein-tagged oligonucleotide. Confocal images were taken of larger cells close to the main vein (left) or of cells at the center of the leaf (right). Cells were imaged using fluorescein isothiocyanate and tetramethylrhodamine isothiocynate filters, and these images were merged. Green color corresponds to the location of poly(A) RNA, which accumulates to higher levels in the nuclei of *sar1-1 sar3-1* cells.

the stability of the AXR3/IAA17 protein (Gray et al., 2001). Seedlings were stained for β-glucuronidase (GUS) expression either directly after a 2-h heat shock or 90 min after return to 22°C. The results shown in Figure 8A indicate that *sar1-1* roots exhibit stronger GUS staining than wild-type roots directly after heat shock and after 90 min. To determine the effects of *sar1-1* on the stability of AXR3NT-GUS, GUS activity was measured by 4-methylumbelliferyl-β-D-glucuronide (MUG) assay at intervals after the seedlings were returned to 22°C (Figure 8B). Surprisingly, GUS activity levels in *sar1-1* seedlings at time 0 were consistently lower than those in the wild type (experiment repeated three times), despite the fact that GUS staining was always stronger in the mutant. For the experiment shown, GUS activity at time 0 was 482.9 ± 69.8 and 101.1 ± 17.9 nM MU/µg protein for Col-0 and *sar1-1*, respectively. The reason for this discrepancy is unknown. In any case, when GUS activity was expressed relative to time 0, our results indicate that the fusion protein was more stable in *sar1-1* than in wild-type plants (Figure 8B).

Because the Aux/IAA proteins are repressors of auxin response, we expected their stability to be lower in the suppressors rather than higher. However, a closer examination of the cellular localization of the AXR3NT-GUS protein may resolve this paradox. Consistent with its role as a transcriptional repressor, the Aux/IAA proteins are localized to the nucleus (Oeller and Theologis, 1995; Gray et al., 2001). In wild-type plants, nuclear localization of

AXR3NT-GUS can be clearly observed in Figure 8C. However, in *sar1* and *sar3* mutants, GUS staining was observed throughout the cell, suggesting that SAR1 and SAR3 are required for either nuclear transport or retention of AXR3NT-GUS (Figures 8D and 8E). This staining pattern is dependent on a relatively short incubation of seedlings with the enzyme substrate. After a longer incubation, we observed a broader distribution of GUS staining in wild-type roots as well (Figure 8E). In *axr1(HSAXR3NT-GUS)* roots, the staining pattern was also nucleus-localized after a short incubation time (Figure 8G). However, in the *sar3 axr1* double mutant, the pattern of GUS staining was similar to that observed in the single *sar1* and *sar3* mutants (Figure 8H). This finding indicates that the alteration in AXR3NT-GUS expression in *sar1* and *sar3* is independent of *AXR1*.

DISCUSSION

Despite the importance of nucleocytoplasmic transport for cellular function, almost nothing is known about this process in plants. In this report, we describe the identification and characterization of two putative subunits of the NPC. In animals and yeast, nucleocytoplasmic transport is mediated by the activity of the NPC, carrier proteins termed karyopherins, and the small GTPase Ran (Gorlich and Kutay, 1999). Many NPC subunits are conserved between animals and yeast, indicating that the
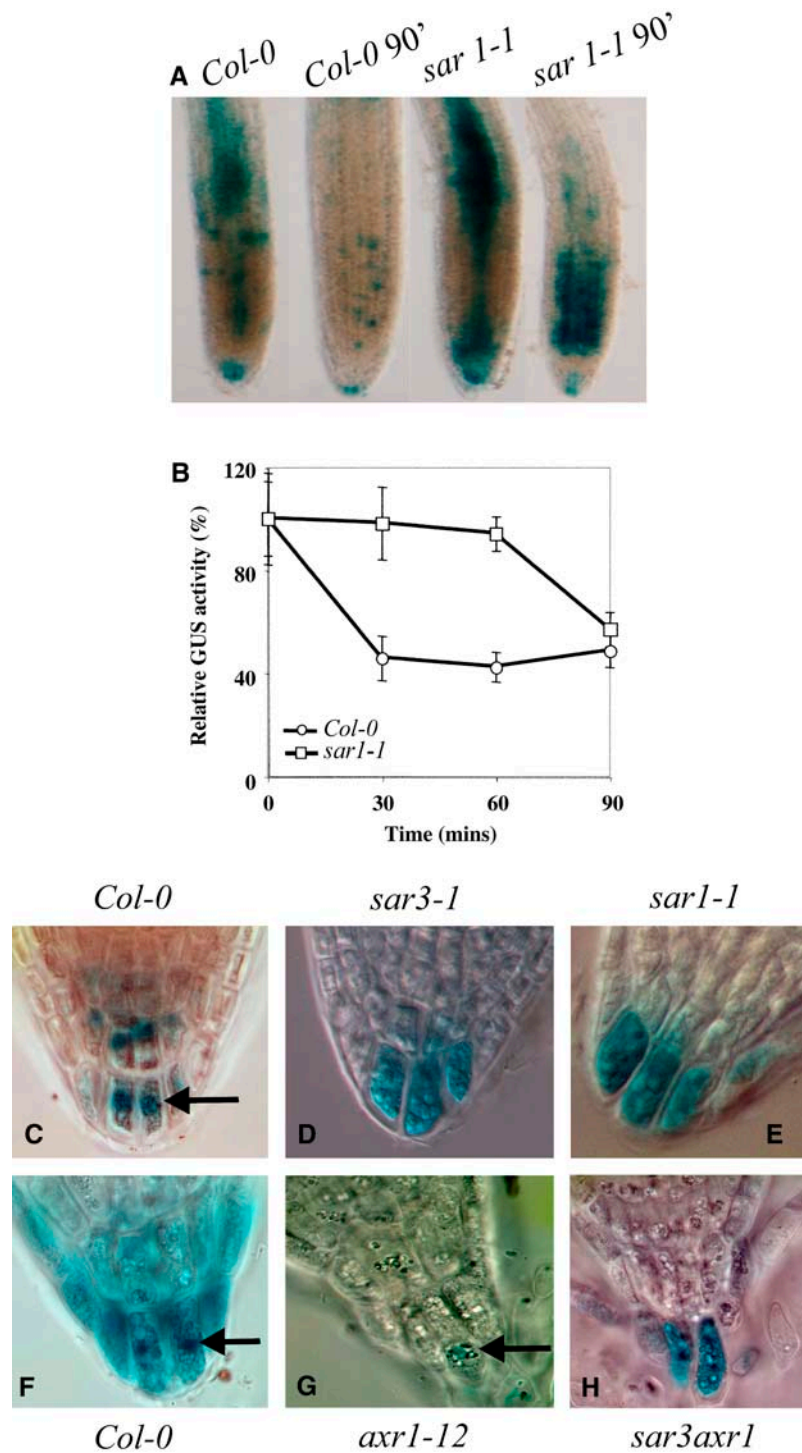
Figure 8. The *sar1* and *sar3* Mutations Affect the Localization of the AXR3NT:GUS Protein.

(A) Seven-day-old *HS:AXR3NT:GUS* seedlings in a wild-type or *sar1* background were heat-shocked at 37°C for 2 h and then placed at 22°C for 90 min. Samples from time 0 or 90 min (90′) were stained with GUS overnight.

(B) Seedlings were treated as described for **(A)**. Protein extracted from seedlings at each time point was tested in a MUG fluorescence assay. The amount of fluorescence produced in each sample was expressed as a percentage of the fluorescence at the end of the heat-shock period. Values reported are means of two determinations. Similar results were obtained in a second, independent experiment.

(C) to **(H)** *HS:AXR3NT:GUS* seedlings in a wild-type or mutant background were heat-shocked at 37°C for 2 h and then stained with GUS solution for 45 min (**[C]** to **[E]**, **[G]**, and **[H]**) or 2 h **(F)**. Images show GUS expression in the root tip region, and arrows indicate the positions of nuclei.

function and overall structure of the NPC are likely to be similar in distantly related eukaryotes (Vasu and Forbes, 2001; Bapteste et al., 2005). The animal NUP107–120 complex comprises at least nine subunits and has been shown to be functionally equivalent to the yeast NUP84 complex (Cronshaw et al., 2002; Lutzmann et al., 2002; Harel et al., 2003; Bai et al., 2004; Loiodice et al., 2004; Bapteste et al., 2005). Our own analysis reveals that most sub-units of the NUP107–120 complex have identifiable homologs in the *Arabidopsis* proteome. These include NUP160, NUP133, NUP107, NUP96, NUP85, NUP43, and two proteins similar to Sec13 (G. Parry and M. Estelle, unpublished data). The presence of many putative NUP107–120 proteins in *Arabidopsis* strongly suggests that the complex exists in a similar form in plants.

We have shown that the SAR1 and SAR3 proteins are related to the human nucleoporins NUP160 and NUP96, respectively. We have demonstrated that *SAR1* and *SAR3/MOS3* are broadly expressed and confirm that SAR3/MOS3 localizes to the nuclear periphery (Zhang and Li, 2005). The *sar1* and *sar3* mutants have a similar pleiotropic phenotype with diverse growth defects, con-firming that the NPC is important for many aspects of plant development. These results also suggest that SAR1 and SAR3/MOS3 have related functions in the NPC. Furthermore, *sar1 sar3* double mutants exhibit a much more severe phenotype than either single mutant, suggesting that the loss of both subunits results in a further decrease in NPC function. Because SAR1 and SAR3/MOS3 may be part of the NUP107–120 subcomplex, this phenotype may be caused by a severe defect in the assembly and/or function of this subcomplex.

The human and yeast homologs of SAR3/MOS3, NUP96 and NUP145C, are present within equivalent NUP subcomplexes (Lutzmann et al., 2002; Harel et al., 2003; Walther et al., 2003; Bai et al., 2004). Most of the investigations regarding the role of vertebrate NUP96 and yeast NUP145C have focused on the proteolytic event that releases NUP98 and NUP96 from the NUP196 polyprotein (or NUP145N and NUP145C from NUP145 in *S. cerevisiae*). Processing of the polyprotein is achieved by an autoproteolytic event that is conserved from yeast to vertebrates (Teixeira et al., 1997, 1999; Fontoura et al., 1999; Rosenblum and Blobel, 1999; Hodel et al., 2002). Failure to process the poly-protein results in severe defects, because the polyprotein is not localized correctly to the nuclear rim (Fontoura et al., 1999). SAR3/MOS3 is translated as a single polypeptide that is similar to vertebrate NUP96. However, examination of the N-terminal region of SAR3/MOS3 reveals that it has similarity to the C-terminal region of vertebrate NUP98. This region contains the peptide motif that is necessary for the autoproteolytic cleav-age of NUP196. Interestingly, the *Arabidopsis* genome encodes two proteins (At1g59660 and At1g10390) that are related to the other product of autoproteolysis, NUP98. These proteins contain the functionally important FG repeats in their N-terminal regions but also contain the proteolytic motif at their C termini. Thus, in *Arabidopsis*, NUP96 and NUP98 are synthesized as distinct peptides that retain the proteolytic motif at their N and C termini, respectively. The N-terminal region of SAR3/MOS3 shares 45% identity with the catalytic region of NUP196 and contains the conserved residues that are necessary for cleavage in verte-brates (Rosenblum and Blobel, 1999; Hodel et al., 2002). Further studies are required to determine whether SAR3/MOS3 un-

dergoes processing to release a short N-terminal peptide and whether this processing is important for function.

Comprehensive analyses of the NUP107–120 complex in *S. cerevisiae*, *Schizosaccharomyces pombe*, *Caenorhabditis ele-gans*, and vertebrate cell culture systems have demonstrated many aspects of its cellular function (Lutzmann et al., 2002; Galy et al., 2003; Harel et al., 2003; Walther et al., 2003; Bai et al., 2004; Loiodice et al., 2004). When the function of the NUP107–120 complex is compromised, it results in a reduction in the nuclear export of RNA irrespective of the organism of study (Aitchison et al., 1995; Vasu et al., 2001; Bai et al., 2004; O'Hagan and Ljungman, 2004). Similarly, we found increased accumula-tion of mRNA in the nucleus of *sar1 sar3* cells relative to wild-type cells, suggesting that there is a defect in mRNA export in these plants. It is difficult to assess the precise developmental conse-quences of nuclear mRNA accumulation, although it is clearly associated with significant growth defects. Severe defects are also observed in the *los4* mutant that accumulate mRNA in the nucleus in a similar manner (Gong et al., 2005).

The *sar1-1* and *sar3-1* mutations suppress auxin resistance in both the *axr1* and *rce1* mutants. This suppression does not appear to involve a direct effect on the RUB conjugation path-way, because neither mutation alters the level of RUB-CUL1. An alternative model is that suppression involves changes in the transport of auxin response proteins, such as the Aux/IAAs. Our data suggest that AXR3NT-GUS is stabilized in *sar1-1* but that this change is related to decreased translocation of the fusion protein into the nucleus rather than to a direct effect on the degradation machinery. If this model is correct, we expect other members of the Aux/IAA protein family to be similarly affected. An overall decrease in the level of these transcriptional repres-sors in the nucleus could explain the partial suppression of the phenotype conferred by *axr1*. However, it is important to note that we did not observe auxin hypersensitivity in *sar1* or *sar3* plants, possibly because other regulatory processes compen-sate for the change in Aux/IAA distribution.

A number of auxin signaling and response genes are targets of miRNAs. The expression of some *AUXIN RESPONSE FACTOR* genes is modulated by the activity of *mi160*, and the *TIR1/AFB* family of auxin receptors are targets of *mi393* (Jones-Rhoades and Bartel, 2004; Mallory et al., 2005; Wang et al., 2005; Navarro et al., 2006). Because SAR1 and SAR3/MOS3 are involved in the nuclear export of RNA, it is possible that the regulation of these genes by miRNAs is affected in *sar1* and *sar3* plants. We examined the *TIR1* transcript level by RT-PCR and found that it was not altered by either mutation (G. Parry and M. Estelle, unpublished data). However, it remains possible that the ex-pression of other miRNA target genes is altered in the mutants.

The effects of mutations in components of the NUP107–120 complex vary in severity depending on the organism. In *C. ele-gans*, reduced levels of *Ce NUP160* (the *SAR1* homolog) result in nearly 100% embryo lethality, whereas the *sar1* mutants are relatively robust. Although this may reflect differences in the importance of these proteins to NPC function, it is also possible that none of the *sar1* or *sar3* mutations are null. In any case, the severe phenotype of the *sar1 sar3* double mutant suggests that the NUP107–120 complex, assuming that this complex is pre-sent in plants, has an important role in NPC function. We have

demonstrated that the *sar1* and *sar3* mutants are deficient in aspects of protein import and RNA export. Based on the phenotypes observed in *sar1*, *sar3*, and double mutant plants, it is likely that these defects affect diverse signaling pathways. In the future, it will be important to determine the functions of SAR1 and SAR3 in the NPC and the precise role of the complex in cellular regulation.

METHODS

Plant Growth Conditions

Plant growth conditions and morphological analyses were as described previously (Lincoln et al., 1990; Cernac et al., 1997). The auxin root elongation assay was performed by growing plants for 4 d on *Arabidopsis thaliana* solution (ATS) followed by transfer onto fresh ATS with or without auxin. Root growth was measured after an additional 3 d and expressed as a proportion of root growth on ATS medium without auxin. Lateral root number in 10-d-old seedlings was determined by scoring emerged primordia using a Nikon SMZ1500 microscope. ATS medium consists of 1% sucrose, 5 mM KNO_3, 2.5 mM KPO_4, 2 mM $MgSO_4$, 2 mM $Ca(NO_3)_2$, 50 μM Fe-EDTA, and 1 mL of micronutrients.

Genetic Analyses

A population of γ-mutagenized *axr1-3* seeds was prepared as described previously (Ruegger et al., 1997). M2 seedlings were screened at 29°C in constant light at an intensity of 85 μE·m^{-2}·s^{-1}. Seedlings with long hypocotyls were selected for further analysis (Gray et al., 1998). The genetic basis for the long-hypocotyl phenotype was determined by backcrossing to *axr1-3* plants and analyzing the F1 and F2 generations. To map the *SAR3* gene, *sar3-1* plants were crossed to Landsberg *erecta* plants and homozygous *sar3-1* plants were identified in the F2 population. By analyzing 680 mutant plants using a variety of CAPS and insertion/deletion PCR-based markers, *sar3* was mapped distal to CAPS marker *g17311* on chromosome 1 on BAC T21F11 or F23A5. After identification of SAR3, PSI-BLAST analysis revealed that SAR3 is homologous with human NUP196 (accession number AAL56659) and yeast NUP145 (accession number CAA96798).

The *sar1-1* gene had been mapped previously between markers *nga280* and *nga248* on chromosome 1 (Cernac et al., 1997). Using an additional population of 647 F2 *sar1-1* plants, we mapped the gene to a 180-kb region on BACs T9L6, T16O9, and F10C21. After the identification of *SAR3*, PSI-BLAST analysis of genes within this interval indicated that At1g33410 is related to human NUP160 (accession number NP_056046). Protein alignments were performed using ClustalX (Chenna et al., 2003).

Protein and RNA Expression

Seedlings were grown for 10 d on agar plates and then transferred to liquid ATS for 1 h with or without 20 μM 2,4-D. RNA was extracted using the Qiagen Plant RNeasy kit, and the RT reaction was conducted on 1 μg of RNA using SuperscriptII RT (Invitrogen). Subsequent PCRs were conducted using 24 cycles (for IAA1 reaction) or 28 cycles in an Eppendorf mastercycler. We used the following primers in RT reactions: SAR1AF, 5′-ATGGAGGAGAATCGTCGGAA-3′; SAR1AR, 5′-TGTATCATCACG-CAGCTCCT-3′; SAR1B, 5′-GGTGAGGCATTATCTGAT-3′; SAR1BR, 5′-AGCGTCTTAGCAGTGAAGAA-3′; SAR1CF, 5′-AAGGCTTTGCACA-GCTTGTC-3′; SAR1CR, 5′-ATCAATGCAACTCTTCTCCC-3′; SAR3AF, 5′-CCGCTTGCTTTGCTGGAGTA-3′; SAR3AR, 5′-TTCACATCCTGCAT-CACGTC-3′; SAR3BF, 5′-TGATGAAGGACCTGCAGA-3′; SAR3BR, 5′-CTAAGCTGAGACCCGGCCCG-3′; IAA1F, 5′-CCTCCTGCAAAAAC-

ACAAATCGTT-3′; IAA1R, 5′-ACAATGGATCATAAGGCAGTAGGA-3′; IAA5F, 5′-TGGCGAATGAGAGTAATAATCTTGGACTCG-3′; IAA5R, 5′-TGGTA-CACATTCACTTTCCTTCAACGTATCAC-3′; ACTINF, 5′-GGGTGAGGC-TGATGATATTC-3′; ACTINR, 5′-TCTGTGAACGATTCCTGGAC-3′.

For cullin protein gel blots, protein was extracted from 10 mg of floral tissue in extraction buffer (125 mM Tris, pH 8.8, 1% SDS, 10% glycerol, and 50 mM $Na_2S_2O_3$). For analysis of GFP expression, protein was extracted from 9-d-old seedlings in extraction buffer (100 mM Tris, pH 7.5, 150 mM NaCl, 1 mM phenylmethylsulfonyl fluoride, 0.1% Tween, and a Complete mini protease inhibitor tablet [1 tablet/10 mL; Roche]). GFP (30 μg) or cullin (50 μg) total protein was subjected to SDS-PAGE and blotted onto a polyvinylidene difluoride membrane (Bio-Rad). The blot was probed with rabbit anti-GFP or rabbit anti-CUL1 antibody (del Pozo and Estelle, 1999) and was visualized using the ECL system (Amersham).

Analysis of GUS Expression

Transgenic *HS:AXR3NT:GUS* seedlings were grown for 5 to 7 d on ATS medium and then transferred to liquid ATS for a 2-h heat shock at 37°C. Seedlings were then either left at 22°C for 90 min or immediately stained in X-Gluc staining solution for between 45 min and overnight [X-Gluc staining solution consists of 0.05 M Na phosphate buffer, pH 7.2, 10 mM $K_4Fe(CN)_6$, 10 mM $K_3Fe(CN)_6$, 0.1% Triton X-100, and 1 mM 5-bromo-4-chloro-3-indolyl-β-D-glucuronide]. Roots were cleared using a decreasing ethanol series, and root tips were mounted in 50% glycerol. Images were obtained on a Nikon E800 microscope.

For quantitative MUG assays, transgenic *HS:AXR3NT:GUS* seedlings were heat-shocked as described above. After heat shock, 10 to 15 seedlings were held at 22°C for appropriate times and then frozen in liquid N_2. Protein was then extracted in MUG extraction buffer (50 mM Na phosphate buffer, pH 7.0, 0.1% Sarkosyl, 0.1% Triton X-100, 10 mM β-mercaptoethanol, and 10 mM EDTA), and protein concentrations were determined by Bradford assay. The MUG assay was conducted using 50 μg of protein incubated for 16 h at room temperature in MUG reaction buffer (extraction buffer + 2 mM MUG), and the reaction was stopped in 10× 0.2 M $NaCO_3$. Fluorescence was measured using a TKO 100 fluorometer (Hoefer Scientific), calculated as nanomolar MU per microgram of protein and represented as a percentage of the expression at the end of the heat shock. Experiments were performed in duplicate and the values averaged.

DNA Constructs

The *PRE/SAR3* cDNA in pBluescript was a kind gift from Jose Martinez-Zapater. To generate the *35S:SAR3-GFP* construct, the *SAR3* cDNA was amplified and cloned into pENTR/D-TOPO using standard Gateway protocols (Invitrogen) (primers N96entrF [5′-CACCATGACGTCTCTTTC-TATTCAACC-3′] and N96entrNSR [5′-AGCTGAGATTTGGCCCGTCTC-3′]). *SAR3* was then moved by LR clonase reaction into destination vector pVR-GFPCt (a kind gift from Vincent Rubio). Constructs were electroporated into *Agrobacterium tumefaciens* strain GV3101, and plant transformation was performed by floral dip (Clough and Bent, 1998). Transformants were selected on ATS plates with 200 mg/mL gentamycin (*pVR-SAR-GFP*). GFP expression was visualized on a Leica TCS SP confocal microscope using the green laser (500 to 550 nm) and viewed through the fluorescein isothiocyanate filter. Cell walls were visualized by staining seedlings with 1 μg/mL propidium iodide in water for 1 min and then washed in water for 5 min.

Whole-Mount in Situ Localization of mRNA

The procedure for in situ localization of mRNA was modified from Gong et al. (2005). Small leaves (<5 mm) were taken from wild-type and *sar1*

sar3 plants and fixed for 30 min with gentle agitation in 1:1 fixation buffer:heptane (fixation buffer consists of 120 mM NaCl, 7 mM Na_2HPO_4, 3 mM NaH_2PO_4, 2.7 mM KCl, 40 mM EGTA, 0.1% Tween 20, 10% DMSO, and 5% formaldehyde [FA]). Samples were washed for 5 min twice in methanol and three times in 100% ethanol before incubation for 30 min in 1:1 ethanol:xylene. Samples were then washed for 5 min twice with ethanol, once with methanol, and once with methanol:fixation buffer (−FA) and postfixed in fixation buffer (+FA) for 30 min. After fixation, leaves were rinsed for 5 min twice with fixation buffer (−FA) and then once in 1% blocking reagent in fixation buffer (−FA) (Roche 1 093 657). Samples were then blocked for 1 h at 50°C in 2 mL of 1% blocking buffer before addition of 1 μg of 50-mer oligo(dT) with a 5′ fluorescein tag (synthesized by Gibco BRL) and incubated overnight at 50°C. Samples were mounted in water and viewed using a Leica TCS SP confocal microscope. Equivalent laser intensity was used for each set of wild-type and *sar1 sar3* samples. Samples were excited at 450 to 500 nm and 530 to 580 nm, and images were taken using fluorescein isothiocyanate and tetramethylrhodamine isothiocynate filters. Samples were viewed with a ×63 objective, and images were generated by collection of 9 to 12 optical sections of 0.7 μm.

Accession Numbers

Sequence data for the main genes discussed in this article can be found in the GenBank/EMBL data libraries under accession numbers At1g33410 (*SAR1*) and At1g10860 (*SAR3*). The putative *Arabidopsis* homologs of known vertebrate nucleoporins are listed in the data libraries as follows: NUP133, At2g05120; NUP107, At3g14120; NUP85, At4g32910.1; NUP43, At4g30840; Sec13, At2g30050 and At3g01340.

Supplemental Data

The following materials are available in the online version of this article.

   Supplemental Figure 1. The *sar3* Mutation Suppresses the Resistance of *axr1* to Methyl Jasmonate.

   Supplemental Figure 2. *sar rce1* Seedlings Have a Different Phenotype Than *rce1* Seedlings.

   Supplemental Figure 3. The SAR3 Protein Is Similar to Yeast NUP145.

REFERENCES

Abel, S., Nguyen, M.D., and Theologis, A. (1995). The PS-IAA4/5-like family of early auxin-inducible mRNAs in *Arabidopsis thaliana.* J. Mol. Biol. **251,** 533–549.

Aitchison, J.D., Blobel, G., and Rout, M.P. (1995). Nup120p: A yeast nucleoporin required for NPC distribution and mRNA transport. J. Cell Biol. **131,** 1659–1675.

Alonso, J.M., et al. (2003). Genome-wide insertional mutagenesis of *Arabidopsis thaliana.* Science **301,** 653–657.

Bai, S.W., Rouquette, J., Umeda, M., Faigle, W., Loew, D., Sazer, S., and Doye, V. (2004). The fission yeast Nup107–120 complex functionally interacts with the small GTPase Ran/Spi1 and is required for mRNA export, nuclear pore distribution, and proper cell division. Mol. Cell. Biol. **24,** 6379–6392.

Bapteste, E., Charlebois, R.L., MacLeod, D., and Brochier, C. (2005). The two tempos of nuclear pore complex evolution: Highly adapting proteins in an ancient frozen structure. Genome Biol. **6,** R85.

Boehmer, T., Enninga, J., Dales, S., Blobel, G., and Zhong, H. (2003). Depletion of a single nucleoporin, Nup107, prevents the assembly of a subset of nucleoporins into the nuclear pore complex. Proc. Natl. Acad. Sci. USA **100,** 981–985.

Bollman, K.M., Aukerman, M.J., Park, M.Y., Hunter, C., Berardini, T.Z., and Poethig, R.S. (2003). HASTY, the Arabidopsis ortholog of exportin 5/MSN5, regulates phase change and morphogenesis. Development **130,** 1493–1504.

Cernac, A., Lincoln, C., Lammer, D., and Estelle, M. (1997). The SAR1 gene of Arabidopsis acts downstream of the AXR1 gene in auxin response. Development **124,** 1583–1591.

Chenna, R., Sugawara, H., Koike, T., Lopez, R., Gibson, T.J., Higgins, D.G., and Thompson, J.D. (2003). Multiple sequence alignment with the Clustal series of programs. Nucleic Acids Res. **31,** 3497–3500.

Clough, S.J., and Bent, A.F. (1998). Floral dip: A simplified method for Agrobacterium-mediated transformation of *Arabidopsis thaliana.* Plant J. **16,** 735–743.

Cronshaw, J.M., Krutchinsky, A.N., Zhang, W., Chait, B.T., and Matunis, M.J. (2002). Proteomic analysis of the mammalian nuclear pore complex. J. Cell Biol. **158,** 915–927.

del Pozo, J.C., Dharmasiri, S., Hellmann, H., Walker, L., Gray, W.M., and Estelle, M. (2002). AXR1–ECR1-dependent conjugation of RUB1 to the Arabidopsis cullin AtCUL1 is required for auxin response. Plant Cell **14,** 421–433.

del Pozo, J.C., and Estelle, M. (1999). The Arabidopsis cullin AtCUL1 is modified by the ubiquitin-related protein RUB1. Proc. Natl. Acad. Sci. USA **96,** 15342–15347.

Deshaies, R.J. (1999). SCF and cullin/ring H2-based ubiquitin ligases. Annu. Rev. Cell Dev. Biol. **15,** 435–467.

Dharmasiri, N., and Estelle, M. (2004). Auxin signaling and regulated protein degradation. Trends Plant Sci. **9,** 302–308.

Dharmasiri, S., Dharmasiri, N., Hellmann, H., and Estelle, M. (2003). The RUB/Nedd8 conjugation pathway is required for early development in Arabidopsis. EMBO J. **22,** 1762–1770.

Enninga, J., Levay, A., and Fontoura, B.M. (2003). Sec13 shuttles between the nucleus and the cytoplasm and stably interacts with Nup96 at the nuclear pore complex. Mol. Cell. Biol. **23,** 7271–7284.

Fabre, E., Boelens, W.C., Wimmer, C., Mattaj, I.W., and Hurt, E.C. (1994). Nup145p is required for nuclear export of mRNA and binds homopolymeric RNA in vitro via a novel conserved motif. Cell **78,** 275–289.

Fontoura, B.M., Blobel, G., and Matunis, M.J. (1999). A conserved biogenesis pathway for nucleoporins: Proteolytic processing of a 186-kilodalton precursor generates Nup98 and the novel nucleoporin, Nup96. J. Cell Biol. **144,** 1097–1112.

Galy, V., Mattaj, I.W., and Askjaer, P. (2003). *Caenorhabditis elegans* nucleoporins Nup93 and Nup205 determine the limit of nuclear pore complex size exclusion in vivo. Mol. Biol. Cell **14,** 5104–5115.

Gong, Z., Dong, C.H., Lee, H., Zhu, J., Xiong, L., Gong, D., Stevenson, B., and Zhu, J.K. (2005). A DEAD box RNA helicase is essential for mRNA export and important for development and stress responses in *Arabidopsis.* Plant Cell **17,** 256–267.

Gorlich, D., and Kutay, U. (1999). Transport between the cell nucleus and the cytoplasm. Annu. Rev. Cell Dev. Biol. **15,** 607–660.

Gray, W.M., del Pozo, J.C., Walker, L., Hobbie, L., Risseeuw, E., Banks, T., Crosby, W.L., Yang, M., Ma, H., and Estelle, M. (1999). Identification of an SCF ubiquitin-ligase complex required for auxin response in *Arabidopsis thaliana.* Genes Dev. **13,** 1678–1691.

Gray, W.M., Kepinski, S., Rouse, D., Leyser, O., and Estelle, M. (2001). Auxin regulates SCF(TIR1)-dependent degradation of AUX/IAA proteins. Nature **414,** 271–276.

Gray, W.M., Ostin, A., Sandberg, G., Romano, C.P., and Estelle, M. (1998). High temperature promotes auxin-mediated hypocotyl elongation in Arabidopsis. Proc. Natl. Acad. Sci. USA **95,** 7197–7202.

Harel, A., and Forbes, D.J. (2004). Importin beta: Conducting a much larger cellular symphony. Mol. Cell **16,** 319–330.

Harel, A., Orjalo, A.V., Vincent, T., Lachish-Zalait, A., Vasu, S., Shah, S., Zimmerman, E., Elbaum, M., and Forbes, D.J. (2003). Removal of a single pore subcomplex results in vertebrate nuclei devoid of nuclear pores. Mol. Cell **11,** 853–864.

Hetzer, M.W., Walther, T.C., and Mattaj, I.W. (2005). Pushing the envelope: Structure, function, and dynamics of the nuclear periphery. Annu. Rev. Cell Dev. Biol. **21,** 347–380.

Hodel, A.E., Hodel, M.R., Griffis, E.R., Hennig, K.A., Ratner, G.A., Xu, S., and Powers, M.A. (2002). The three-dimensional structure of the autoproteolytic, nuclear pore-targeting domain of the human nucleoporin Nup98. Mol. Cell **10,** 347–358.

Hunter, C.A., Aukerman, M.J., Sun, H., Fokina, M., and Poethig, R.S. (2003). PAUSED encodes the Arabidopsis exportin-t ortholog. Plant Physiol. **132,** 2135–2143.

Jones-Rhoades, M.W., and Bartel, D.P. (2004). Computational identification of plant microRNAs and their targets, including a stress-induced miRNA. Mol. Cell **14,** 787–799.

Leyser, H.M., Lincoln, C.A., Timpte, C., Lammer, D., Turner, J., and Estelle, M. (1993). Arabidopsis auxin-resistance gene AXR1 encodes a protein related to ubiquitin-activating enzyme E1. Nature **364,** 161–164.

Li, J., and Chen, X. (2003). PAUSED, a putative exportin-t, acts pleiotropically in Arabidopsis development but is dispensable for viability. Plant Physiol. **132,** 1913–1924.

Lincoln, C., Britton, J.H., and Estelle, M. (1990). Growth and development of the axr1 mutants of Arabidopsis. Plant Cell **2,** 1071–1080.

Loiodice, I., Alves, A., Rabut, G., Van Overbeek, M., Ellenberg, J., Sibarita, J.B., and Doye, V. (2004). The entire Nup107–160 complex, including three new members, is targeted as one entity to kinetochores in mitosis. Mol. Biol. Cell **15,** 3333–3344.

Lutzmann, M., Kunze, R., Buerer, A., Aebi, U., and Hurt, E. (2002). Modular self-assembly of a Y-shaped multiprotein complex from seven nucleoporins. EMBO J. **21,** 387–397.

Mallory, A.C., Bartel, D.P., and Bartel, B. (2005). MicroRNA-directed regulation of *Arabidopsis* AUXIN RESPONSE FACTOR17 is essential for proper development and modulates expression of early auxin response genes. Plant Cell **17,** 1360–1375.

Meier, I. (2005). Nucleocytoplasmic trafficking in plant cells. Int. Rev. Cytol. **244,** 95–135.

Merkle, T. (2003). Nucleo-cytoplasmic partitioning of proteins in plants: Implications for the regulation of environmental and developmental signalling. Curr. Genet. **44,** 231–260.

Moon, J., Parry, G., and Estelle, M. (2004). The ubiquitin-proteasome pathway and plant development. Plant Cell **16,** 3181–3195.

Mosammaparast, N., and Pemberton, L.F. (2004). Karyopherins: From nuclear-transport mediators to nuclear-function regulators. Trends Cell Biol. **14,** 547–556.

Navarro, L., Dunoyer, P., Jay, F., Arnold, B., Dharmasiri, N., Estelle, M., Voinnet, O., Jones, J.D. (2006). A plant miRNA contributes to antibacterial resistance by repressing auxin signaling. Science **312,** 436–439.

Oeller, P.W., and Theologis, A. (1995). Induction kinetics of the nuclear proteins encoded by the early indoleacetic acid-inducible genes, PS-IAA4/5 and PS-IAA6, in pea (*Pisum sativum* L.). Plant J. **7,** 37–48.

O'Hagan, H.M., and Ljungman, M. (2004). Efficient NES-dependent protein nuclear export requires ongoing synthesis and export of mRNAs. Exp. Cell Res. **297,** 548–559.

Palma, K., Zhang, Y., and Li, X. (2005). An importin alpha homolog, MOS6, plays an important role in plant innate immunity. Curr. Biol. **15,** 1129–1135.

Park, M.Y., Wu, G., Gonzalez-Sulser, A., Vaucheret, H., and Poethig, R.S. (2005). Nuclear processing and export of microRNAs in Arabidopsis. Proc. Natl. Acad. Sci. USA **102,** 3691–3696.

Parry, G., and Estelle, M. (2004). Regulation of cullin-based ubiquitin ligases by the Nedd8/RUB ubiquitin-like proteins. Semin. Cell Dev. Biol. **15,** 221–229.

Rosenblum, J.S., and Blobel, G. (1999). Autoproteolysis in nucleoporin biogenesis. Proc. Natl. Acad. Sci. USA **96,** 11370–11375.

Ruegger, M., Dewey, E., Hobbie, L., Brown, D., Bernasconi, P., Turner, J., Muday, G., and Estelle, M. (1997). Reduced naphthylphthalamic acid binding in the tir3 mutant of Arabidopsis is associated with a reduction in polar auxin transport and diverse morphological defects. Plant Cell **9,** 745–757.

Siniossoglou, S., Lutzmann, M., Santos-Rosa, H., Leonard, K., Mueller, S., Aebi, U., and Hurt, E. (2000). Structure and assembly of the Nup84p complex. J. Cell Biol. **149,** 41–54.

Siniossoglou, S., Wimmer, C., Rieger, M., Doye, V., Tekotte, H., Weise, C., Emig, S., Segref, A., and Hurt, E.C. (1996). A novel complex of nucleoporins, which includes Sec13p and a Sec13p homolog, is essential for normal nuclear pores. Cell **84,** 265–275.

Teixeira, M.T., Fabre, E., and Dujon, B. (1999). Self-catalyzed cleavage of the yeast nucleoporin Nup145p precursor. J. Biol. Chem. **274,** 32439–32444.

Teixeira, M.T., Siniossoglou, S., Podtelejnikov, S., Benichou, J.C., Mann, M., Dujon, B., Hurt, E., and Fabre, E. (1997). Two functionally distinct domains generated by in vivo cleavage of Nup145p: A novel biogenesis pathway for nucleoporins. EMBO J. **16,** 5086–5097.

Telfer, A., and Poethig, R.S. (1998). HASTY: A gene that regulates the timing of shoot maturation in *Arabidopsis thaliana.* Development **125,** 1889–1898.

Timpte, C., Lincoln, C., Pickett, F.B., Turner, J., and Estelle, M. (1995). The AXR1 and AUX1 genes of Arabidopsis function in separate auxin-response pathways. Plant J. **8,** 561–569.

Tiryaki, I., and Staswick, P.E. (2002). An Arabidopsis mutant defective in jasmonate response is allelic to the auxin-signaling mutant axr1. Plant Physiol. **130,** 887–894.

Vasu, S., Shah, S., Orjalo, A., Park, M., Fischer, W.H., and Forbes, D.J. (2001). Novel vertebrate nucleoporins Nup133 and Nup160 play a role in mRNA export. J. Cell Biol. **155,** 339–354.

Vasu, S.K., and Forbes, D.J. (2001). Nuclear pores and nuclear assembly. Curr. Opin. Cell Biol. **13,** 363–375.

Walther, T.C., Alves, A., Pickersgill, H., Loiodice, I., Hetzer, M., Galy, V., Hulsmann, B.B., Kocher, T., Wilm, M., Allen, T., Mattaj, I.W., and Doye, V. (2003). The conserved Nup107–160 complex is critical for nuclear pore complex assembly. Cell **113,** 195–206.

Wang, J.W., Wang, L.J., Mao, Y.B., Cai, W.J., Xue, H.W., and Chen, X.Y. (2005). Control of root cap formation by microRNA-targeted auxin response factors in Arabidopsis. Plant Cell **17,** 2204–2216.

Weis, K. (2003). Regulating access to the genome: Nucleocytoplasmic transport throughout the cell cycle. Cell **112,** 441–451.

Zhang, Y., and Li, X. (2005). A putative nucleoporin 96 is required for both basal defense and constitutive resistance responses mediated by *suppressor of npr1-1,constitutive 1.* Plant Cell **17,** 1306–1316.